J-Researchers

Journal of Civil Engineering Researchers

Journal homepage: www.journals-researchers.com

Numerical Investigation of the Effect of Mass Irregularity on Progressive Collapse of RC Buildings

Mahdi Mashhadiyan,[a] Esmaeil Mousapoor ,[a*] Vahid Janalizadeh [a]

[a] *Department of Civil Engineering, Ram.C., Islamic Azad University, Ramsar, Iran*

ABSTRACT

Mass irregularity, which amplifies stress concentrations and torsional demands, substantially increases the risk of progressive collapse in reinforced concrete structures. Improper design and non-uniform mass distribution are key contributors to such failures, highlighting the need for optimized design and targeted strengthening measures. This study investigates the effects of column removal on a two-story RC moment-resisting frame using ABAQUS. A one-third-scale frame was numerically modeled under both regular and irregular quasi-static loading, considering the removal of a corner and a side column. The model was validated against experimental results, and structural performance was assessed in terms of load-bearing capacity, stiffness degradation, and energy absorption. Results show that adjacent columns experience higher stress than the removed column due to rapid load redistribution through surrounding beams and columns. The progressive collapse sensitivity index under vertical and lateral loads reached 76.2% and 78.5% for corner-column removal under irregular loading, compared to 71.6% and 72.2% for side-column removal. These findings indicate heightened vulnerability to progressive collapse for corner-column loss and irregular mass distribution, emphasizing the importance of uniform mass distribution and robust structural design to mitigate progressive failure.

ARTICLE INFO

Received: June 23 , 2026
Accepted: July 29 , 2026

Keywords:
Numerical development
Progressive collapse
Reinforced concrete moment frame
Mass irregularity
ABAQUS

DOI: 10.66224/JCER.8.3.16
DOR: 20.1001.1.22516530.1399.11.4.1.1

1. Introduction

Mass irregularity occurs when the mass distribution on a building's floors is not uniform, resulting in certain stories carrying significantly more mass than others. This irregularity increases torsional demands, amplifies stress concentrations, and compromises structural stability during seismic excitation. The offset between the center of mass and the center of rigidity further increases the likelihood of soft-story development and progressive collapse. Therefore, balanced architectural–structural design, adequate joint strengthening, and comprehensive dynamic analysis are essential to mitigate these risks [1-3]. The vulnerability and resistance of reinforced concrete structures to the gradual spread of failure can be assessed by evaluating progressive collapse criteria. Structural configuration, flexibility, tolerance to chained loads, control of local failure, resistance to unexpected loads, joint stiffness and ductility, safe evacuation potential, failure propagation speed, and repairability are among the criteria that must be met [4].

* Corresponding author. E-mail: Es.Mousapoor@iau.ac.ir

Additionally, real-world cases of progressive collapse such as Ronan Point, Typhoon Plus, the Sampoong Department Store, and 7 World Trade Center underscore the critical influence of mass irregularity, inadequate design practices, uneven load distribution, and deficient structural connections. These failures clearly demonstrate the necessity for precise, code-compliant, and robustness-oriented design strategies to effectively minimize the likelihood of progressive, chain-type failure mechanisms [5]. The collapse of the Champlain Towers South in Florida in 2021 exemplifies how non-uniform mass distribution, inadequate structural detailing, and construction deficiencies—such as insufficient column reinforcement and improper rebar spacing—can trigger progressive collapse and lead to catastrophic consequences. This failure, which resulted in 98 fatalities, highlighted the critical importance of proper design, construction quality control, and long-term maintenance, and subsequently prompted revisions in building standards across the United States [6].

The phenomenon of progressive collapse, characterized by an initial local failure that propagates through the structure, was first introduced by Pearson in 1970 [7] and has since been extensively investigated. Numerous studies, including those by Chopra [8], Kabeyasawa [9], Mohamed [10], and Jankowiak [11], demonstrate the detrimental effects of mass irregularity on structural stability and collapse propagation. Researchers have found that concentrated or asymmetrically distributed mass can significantly modify the dynamic response, intensify stress concentrations, and necessitate localized strengthening [12–14]. These studies further emphasize that combining mass irregularity with other adverse conditions such as geometric deficiencies, stiffness discontinuities, or inadequate connection types creates more hazardous collapse scenarios [15]. Additionally, research by Liu [16], Lekshmi [17], Zhang [18], Christopoulos [19], and Spencer [20] has proposed mitigation strategies including intelligent structural monitoring, hybrid damping systems, optimized mass–stiffness distribution, and enhanced joint detailing to reduce vulnerability associated with mass irregularity. Further investigations by Chopra [21], Lignos [22], and Kewalramani [23] show that complex loading conditions, such as seismic excitation and temperature induced stresses, exacerbate failure mechanisms when mass irregularity is present. Collectively, these findings highlight that careful consideration of mass distribution and the application of advanced engineering solutions during the design phase play a vital role in preventing progressive collapse [5].

In the next stage of the present research, a one-third-scale reinforced concrete moment-resisting frame is tested experimentally by Hua Huang et al. [24] is numerically modeled and subjected to comparable loading scenarios. While the experimental program applied uniformly distributed loads, the numerical investigation conducted herein incorporates both uniform and irregular mass patterns under vertical and lateral loading conditions. Furthermore, unlike the original study, which considered only the removal of a side column, this research also evaluates the consequences of corner-column removal. After validating the finite element model against the experimental results, the structural response will be assessed through the analysis of load–displacement curves and the progressive collapse sensitivity index. Special attention will be given to evaluating changes in load-carrying capacity, stiffness degradation, strength loss, and energy-absorption capacity under different loading scenarios and column-removal conditions, to gain a comprehensive understanding of how these parameters influence the overall structural behavior.

2. Loading Scenario and Model Validation

In this study, ABAQUS software [25] was employed due to the strong capabilities of the finite element method for complex modeling and advanced nonlinear analysis. The modeling workflow included numerical simulation, validation, and convergence evaluation, ensuring high analytical accuracy and improved reliability of the structural performance assessment. To verify the accuracy of the finite element model, a two-story reinforced concrete (RC) moment-resisting frame previously tested by Hua Huang et al. [24] under dynamic and incremental vertical loading was used as the benchmark specimen. This specimen represents a one-third-scale portion of an eight-story RC frame and consists of the first two stories with two bays in the longitudinal direction and one bay in width (Figure 1).

In this study, the structural design was carried out in accordance with the applicable Chinese codes, incorporating a dead load of 5.5 kN/m², a live load of 2 kN/m², soil class II conditions, and a design seismic acceleration of 0.1g. Huang et al. investigated the progressive collapse initiated by the removal of the ground-floor corner column in their experimental program. The beam and column cross-sections in their model were reduced to one-third of the prototype dimensions, and all remaining geometric properties were adopted as summarized in Table 1. Figure 2 presents the detailed configuration of the RC frame, including member dimensions and reinforcement layout, as reported in their study. The slab was constructed with a thickness of 40 mm and reinforced using a mesh of #6 bars spaced at 80 mm.

In the experimental configuration illustrated in Figure 2, three hydraulic jacks were employed to apply constant vertical loads to Columns A, C, and E, with magnitudes of

138, 138, and 203 kN, respectively. A displacement-controlled jack was utilized to impose the primary loading on Column B. The loads associated with Columns D and F were neglected in the test setup, and structural displacements were recorded using linear variable differential transformers (LVDTs). The mechanical properties of the three-dimensional RC frame, including the yield and ultimate strengths of both primary and secondary reinforcement, are summarized in Table 2. The 28-day compressive strength of the concrete was measured to be 27 MPa.

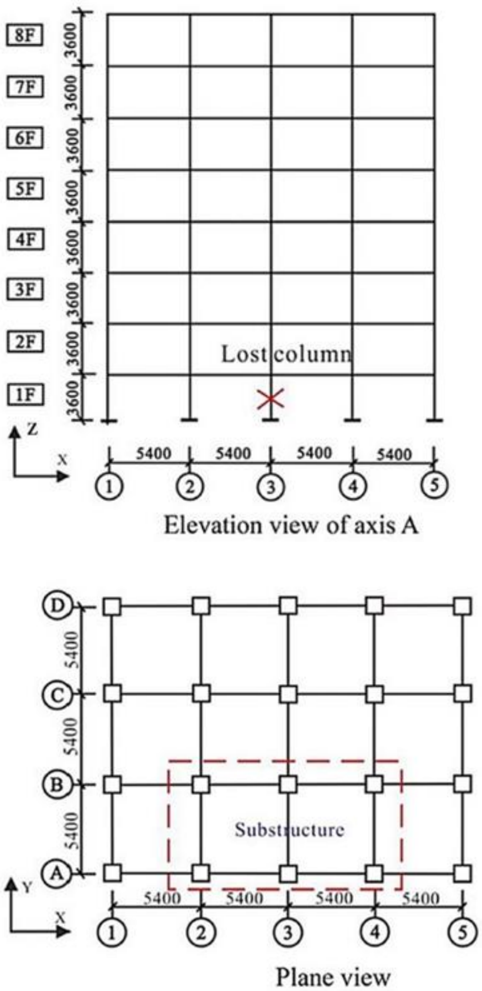

Figure 1. Loading Scenario Introduction: Plan and elevation of a 3D RC frame structure, in which the loss of a corner column on the ground floor, followed by incremental vertical loading in the study by Hua Huang et al., triggers progressive collapse [24].

According to the observations reported by Hua Huang et al. [24], a load–displacement response was recorded during the incremental vertical loading applied to column B. As illustrated in Figure 3, the specimen underwent progressive damage with increasing displacement. At a displacement of 6 mm, ring-shaped and horizontal cracks were first observed. When the displacement reached 14 mm, diagonal cracking developed at the bottom surface of the slab, and by 18 mm, these cracks propagated and interconnected. The test was continued until a displacement of 380 mm, at which point reinforcement rupture occurred, marking the ultimate failure of the specimen.

Table 1.
Dimensional introduction and scale conversion: RC frame structure investigated by Hua Huang et al. [24].

Dimensions	Prototype building (mm)	Test specimens (mm)
Column section (W × D)	600 × 600	200 × 200
Beam section	300 × 600	100 × 200
Slab thickness	120	40
Span length	5400	1800
Concrete cover for columns	45	15
Concrete cover for beams	45	15
Concrete cover for slab	30	10

Table 2.
Material properties used in the 3D RC frame structure, including tensile and ultimate strengths of main and secondary reinforcements.

Types	Yield strength f_y (MPa)	Ultimate strength f_u (MPa)	The strain corresponding to ultimate strength	Elongation (%)
R6	449	541	0.22	23.3
T8	465	555	0.21	22.8
T10	486	567	0.18	20.9
T12	492	627	0.16	17.8

To validate the experimental observations, a numerical model of the two-story RC moment-resisting frame was developed in ABAQUS to reproduce the structural response under vertical loading.

The modeling procedure involved defining and assembling the concrete members and reinforcement, followed by meshing with an optimal element size of 1 cm and assigning the corresponding material properties. The dynamic analysis consisted of two sequential steps: gravity loading and displacement-controlled loading. Reinforcement was modeled using the embedded constraint technique.

Six reference points were created at the column tops and coupled for load application. For simplification, a merge method was adopted in place of tie constraints. As illustrated in Figure 4, a gravity load of 7500 N/m² was applied to the slabs, and a displacement-controlled load of up to 400 mm was incrementally applied to column B, consistent with the experimental procedure reported by Huang et al.

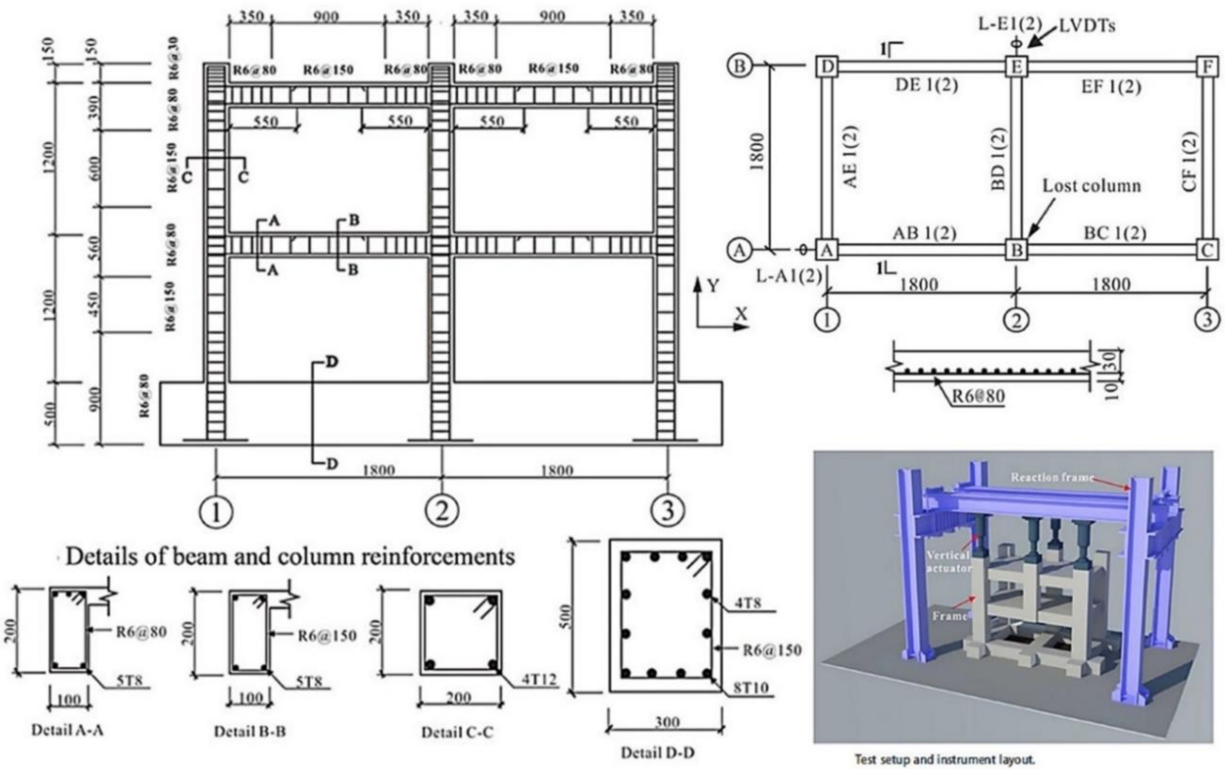

Figure 2. Dimensional details of RC frame structure columns and slab, and loading setup [24].

Figure 3. Damage representation of beams, slabs, and the entire frame due to vertical loading at removed column B in the two-story RC frame studied by Huang et al. [24].

Figure 4 presents the displacement results, while Figure 5 illustrates the corresponding von Mises stress distribution.

Under the initial gravity-loading step, the maximum displacement at the slab center reached 2 mm, and the displacement beneath column B (the removed column) was approximately 1 mm.

During the subsequent displacement-controlled loading, the maximum displacement beneath column B increased to 407 mm. As shown in Figure 5, reinforcement stresses rose to 556 MPa, and the beam B rebars experienced stress-induced damage, resulting in a noticeable reduction in the structural performance.

A vertical load–displacement and numerical reaction curve was obtained from the analysis. For validation, the experimental load–displacement data were digitized and compared with the ABAQUS results. As shown in Figure 6, the maximum resistance and stiffness of the two curves exhibit close agreement, with minor discrepancies attributed to experimental and numerical uncertainties. Furthermore, comparison of damage patterns confirmed consistent load response, demonstrating that the numerical model was successfully validated.

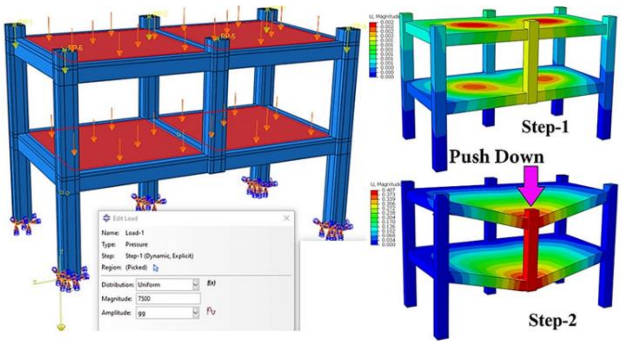

Figure 4. Application of dead and live surface loads as uniformly distributed load on floor slabs, and displacement representation in two analysis steps (gravity and displacement control).

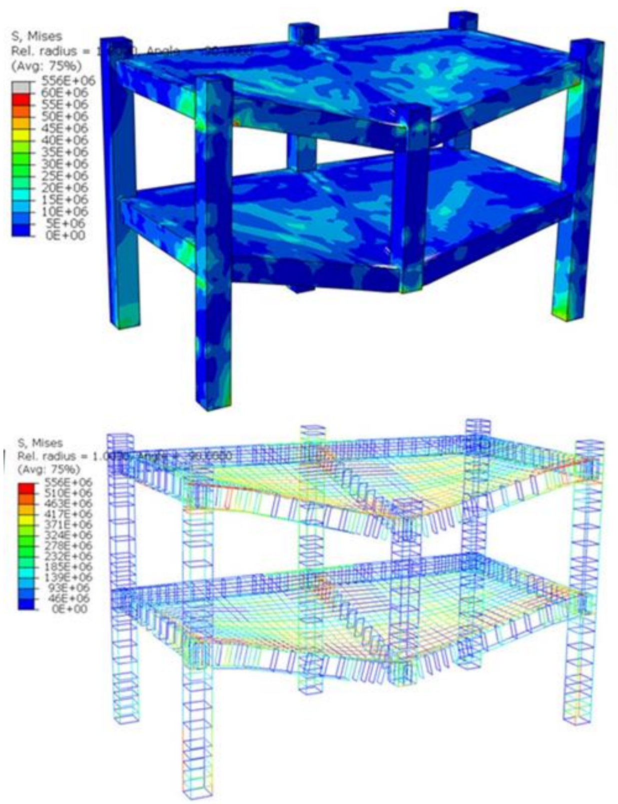

Figure 5. Von Mises stress results for the numerical RC two-story frame structure and reinforcement mesh in ABAQUS.

3. Analysis of Findings

This study examines the seismic response and progressive collapse behavior of a reinforced concrete moment-resisting frame with mass irregularity using finite element modeling in ABAQUS. Following validation of the numerical model against experimental data, the structural performance under vertical and lateral loading is evaluated with emphasis on column-removal location and its influence on collapse sensitivity. The analysis considers four column-removal scenarios (A and B) under both regular and irregular mass distributions. In the nonlinear dynamic phase, the structure is subjected to incrementally increasing displacement-controlled loading, and the resulting pushover curves are used to assess the overall load-bearing capacity before and after column removal. Furthermore, the progressive collapse sensitivity index (SI) is calculated based on the reduction in structural capacity due to column removal, as defined in Equation 1.

Equation1: $SI = (\lambda_0 - \lambda_{damage}) / \lambda 0$

In this equation, λ_0 denotes the total vertical and lateral load-carrying capacity before column removal, while λdamage represents the capacity after removal. The sensitivity index (SI), used to identify critical elements in progressive collapse, is computed from the reduction in structural capacity due to the loss of the column. This index ranges from 0 to 1, with values closer to 1 indicating greater significance of the element and a more severe degradation in overall structural performance upon its removal. To determine the SI for both vertical and lateral loading, four parameters—namely, the load–displacement responses before and after column removal under each loading type—must be evaluated

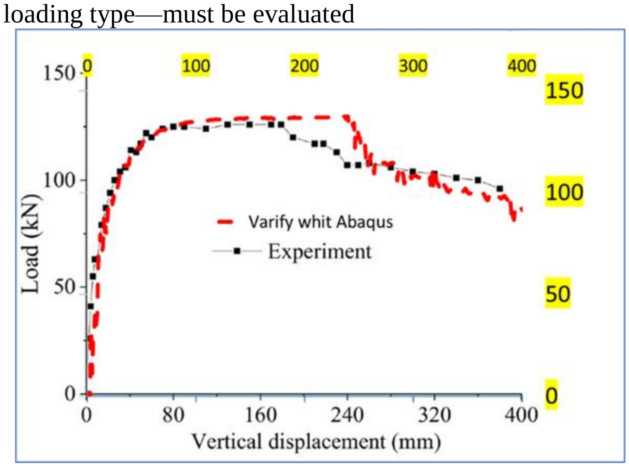

Figure 6. Load-displacement curve comparison between the numerical and experimental two-story RC moment-resisting frame by Huang et al. [24].

3.1. Evaluation of Performance and Sensitivity Index under Regular Mass Load Distribution due to Column B Removal

To evaluate the vertical and lateral performance of the RC moment frame after the removal of column B, the structural response of the intact frame must first be determined under both loading conditions. Accordingly, the undamaged frame is modeled and subjected to vertical and lateral loads to obtain its baseline performance at the location of column B (Figure 7).

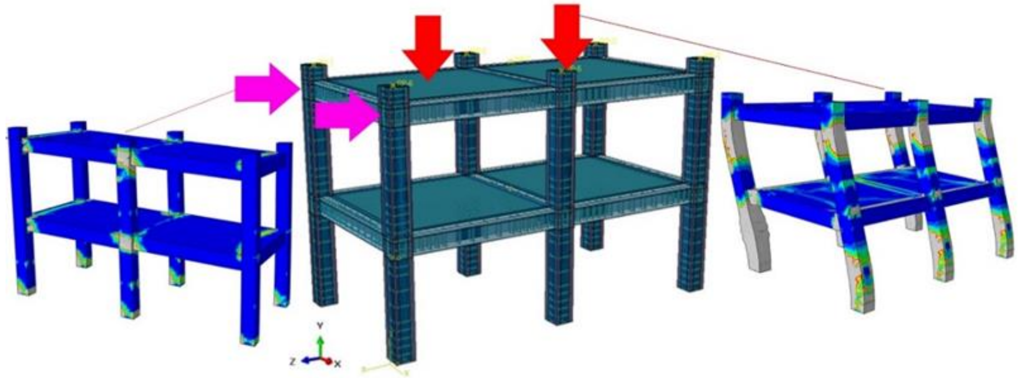

Figure 7. RC moment frame model without column removal using the original reinforcement sample, and results showing deformation under applied vertical and lateral loads.

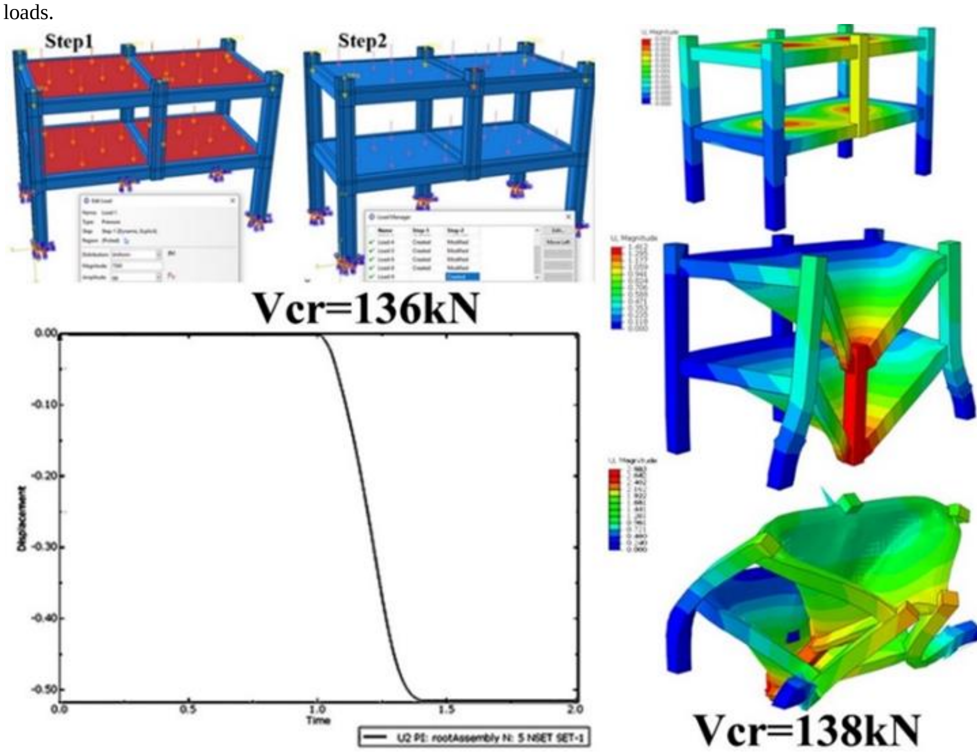

Figure 8. Result of vertical deformation under the critical load applied at the removed column B, and collapse due to loading beyond the critical value.

To assess the structural response after column B removal, the frame was first analyzed in its intact state under vertical and lateral loads to obtain baseline force–displacement data. Subsequently, the post-removal configuration was simulated, applying a vertical load at column B to represent upper-story effects. The force–displacement curves (Figure 6) indicate a critical load of 136 kN, beyond which progressive collapse is initiated, propagating toward the removed column (Figure 8).

After applying the critical load of 136 kN at the location of the removed column B, a vertical displacement of approximately 50 cm was observed, which then stabilized (Figure 8). Subsequently, vertical and lateral loads were applied to the two-story RC frame with regular mass distribution. The resulting force–displacement curves (Figures 9-A and 9-B) were compared to the pre-removal responses. Here, “Full-P” and “Full-L” denote vertical and lateral loading before column removal, respectively, while “B-M-P” and “B-M-L” correspond to vertical and lateral loading after column B removal under regular mass distribution.

From the force–displacement curves, key performance parameters—including strength, stiffness, ductility, and energy absorption—were computed. Vertical (PP) and lateral (PL) strength denote the maximum load capacity, while stiffness was evaluated from the slope of bilinearized force–displacement curves, yielding initial elastic vertical (KP) and lateral (KL) stiffness. Ductility indices (μP and μL) were obtained as the ratio of maximum effective displacement (Δu) to yield displacement (Δy), and the area under the curves provided vertical (EP) and lateral (EL) energy absorption. Using these criteria, the performance of the two-story RC frame with regular mass distribution was assessed before and after column B removal (Figure 9), and the results are summarized in Table 3 and Table 4. The corresponding sensitivity indices under vertical and lateral loading were 62.1% and 65.2%, respectively.

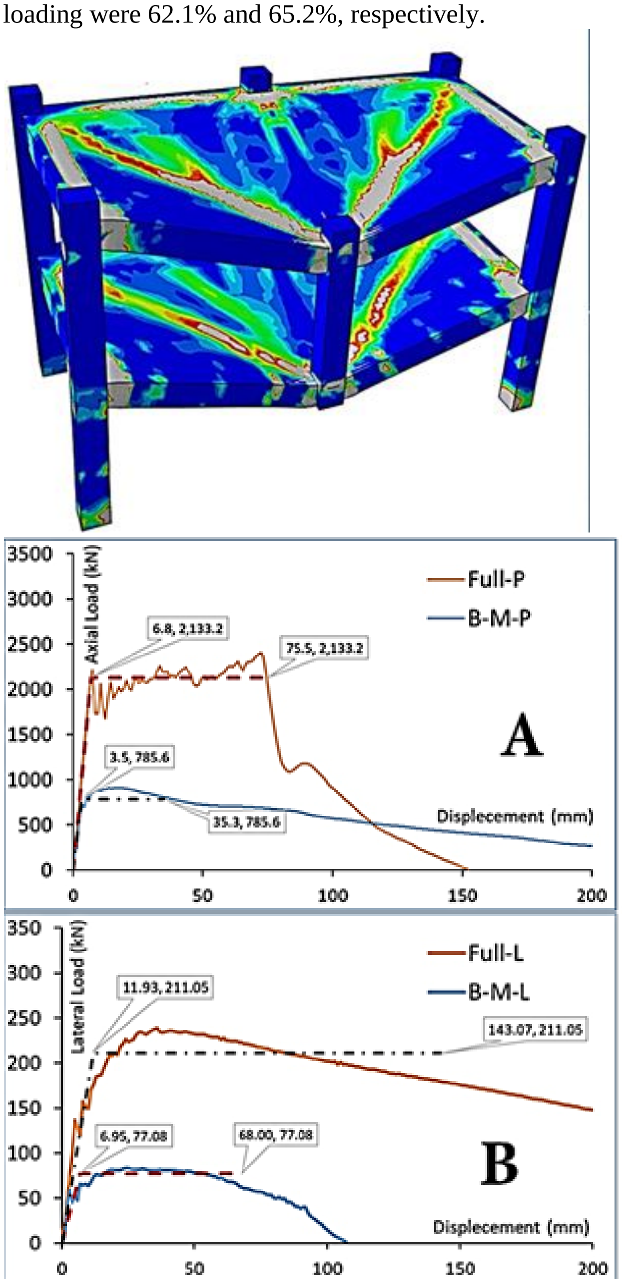

Figure 9. Comparison of vertical and lateral force–displacement curves of a two-story RC moment frame under regular mass distribution before and after column B removal.

3.2. Performance Evaluation and Sensitivity Index under Uniform Mass Load Distribution due to Removal of Column A

This section investigates progressive collapse due to the failure of a corner column instead of a side column. The two-story RC moment-resisting frame from Hua Huang et al. was re-evaluated as both a laboratory and numerical model. Column A1 (Column A) at the ground floor was removed, and the first two stories were analyzed in ABAQUS at one-third scale using displacement-controlled loading with uniformly distributed floor loads. The force–displacement response indicated a critical load of 93.5 kN for the removed column, resulting in the corresponding vertical displacement shown in Figure 11.

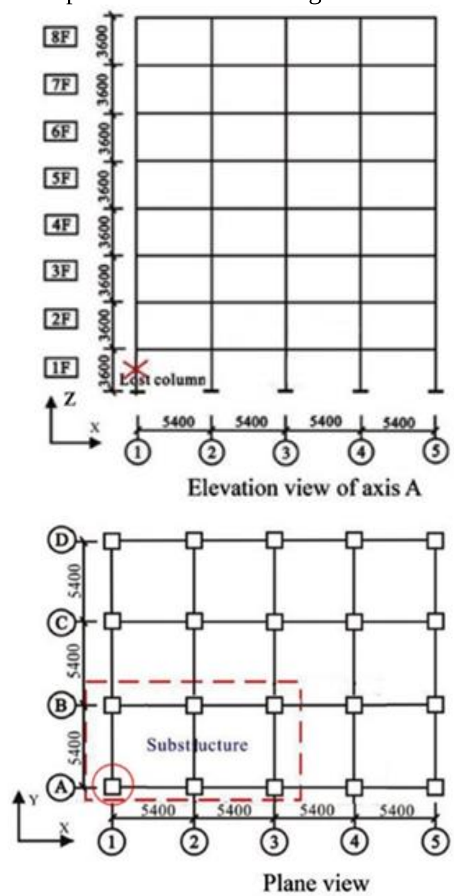

Figure 10. Scenario change in loading: Plan and elevation of the 8-story building with assumed failure at the corner column.

After applying the critical load to the removed corner column A, vertical and lateral loads were applied to the two-story RC frame with uniform mass distribution. The resulting force–displacement curves were compared to the pre-removal responses (Figure 11). Here, “A-M-P” and “A-M-L” denote vertical and lateral load–displacement responses, respectively, after removal of column A.

Table 3.
Results of sensitivity indices and vertical performance of the two-story RC moment frame before and after column removal at position B.

Spectrum	Δ_y (mm)	Δ_u (mm)	Energy E_p (kN*mm)	Reaction Force P_p (kN)	System Hardness K_p (kN/mm)	Ductility μ_p	SI_P
Full-P	6.79	75.46	202843	2407.9	314.4	11.1	62.1%
B-M-P	3.46	35.26	74258	911.7	227.2	10.2	
Change (%)			-63%	-62%	-28%	-8%	

Table 4.
Results of sensitivity indices and lateral performance of the two-story RC moment frame before and after column removal at position B.

Spectrum	Δy (mm)	Δu (mm)	E_l (kN*mm)	P_l (kN)	K_l (kN/mm)	μ_L	SI_L
Full-L	11.93	143.1	38273	239.1	17.7	12.0	65.2%
B-M-L	6.948	68	6455	83.2	11.1	9.8	
Change (%)			-83%	-65%	-37%	-18%	

According to Figure 11, bilinearization of the vertical and lateral load–displacement curves before and after removal of Column A under uniform mass distribution was used to evaluate structural performance. Based on these results, the calculated sensitivity indices for the removed corner column are 63.4% under vertical loading and 69.2% under lateral loading.

3.3. Performance Evaluation and Sensitivity Index under Non-Uniform Mass Load Distribution due to Removal of Column B

In the next stage, the structural performance of the two-story RC moment-resisting frame is evaluated under a non-uniform mass distribution. In this configuration, the second-story load exceeds 50% of the first-story load, as illustrated in Figure 12. The applied floor loads are 6000 N/m² for the first story and 9000 N/m² for the second story, corresponding to a 150% mass ratio. This represents a non-uniform loading condition. After applying vertical and lateral loads and generating the corresponding load–displacement curves, the structural performance and the vertical and lateral sensitivity indices associated with the removal of Column B are evaluated, with the results shown in Figure 12.

According to Figure 12, the vertical and lateral load–displacement responses under the critical load applied at the removed Column B are compared for the intact and damaged states of the two-story RC frame with non-uniform mass distribution. In this figure, B-N-P represents the vertical response and B-N-L represents the lateral response after removal of Column B. The evaluation indicates that the sensitivity indices for vertical and lateral loading under non-uniform mass distribution are 71.6% and 72.2%, respectively.

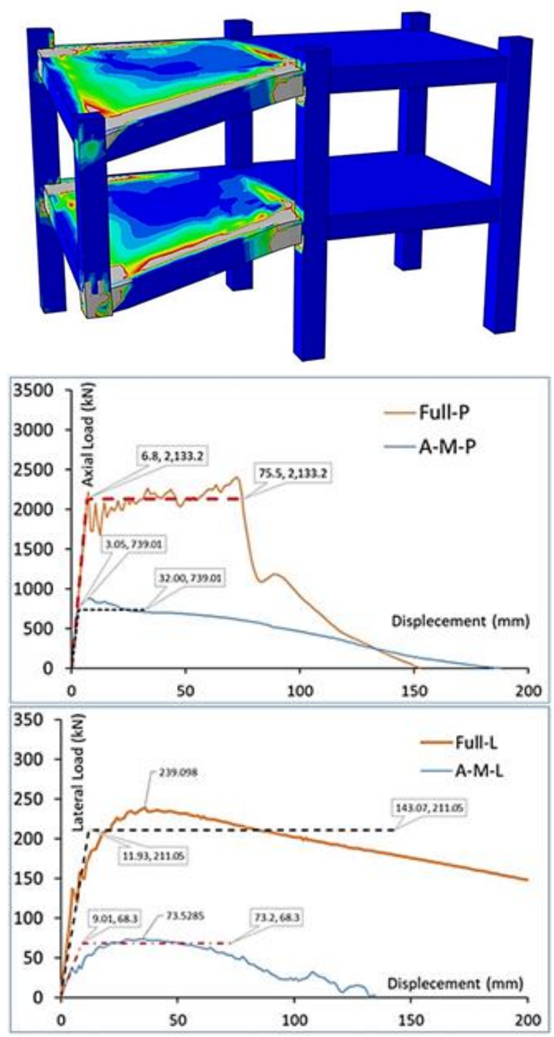

Figure 11. Comparison of vertical and lateral load-displacement curves in the two-story RC moment-resisting frame, under uniform mass load distribution, before and after Column A removal.

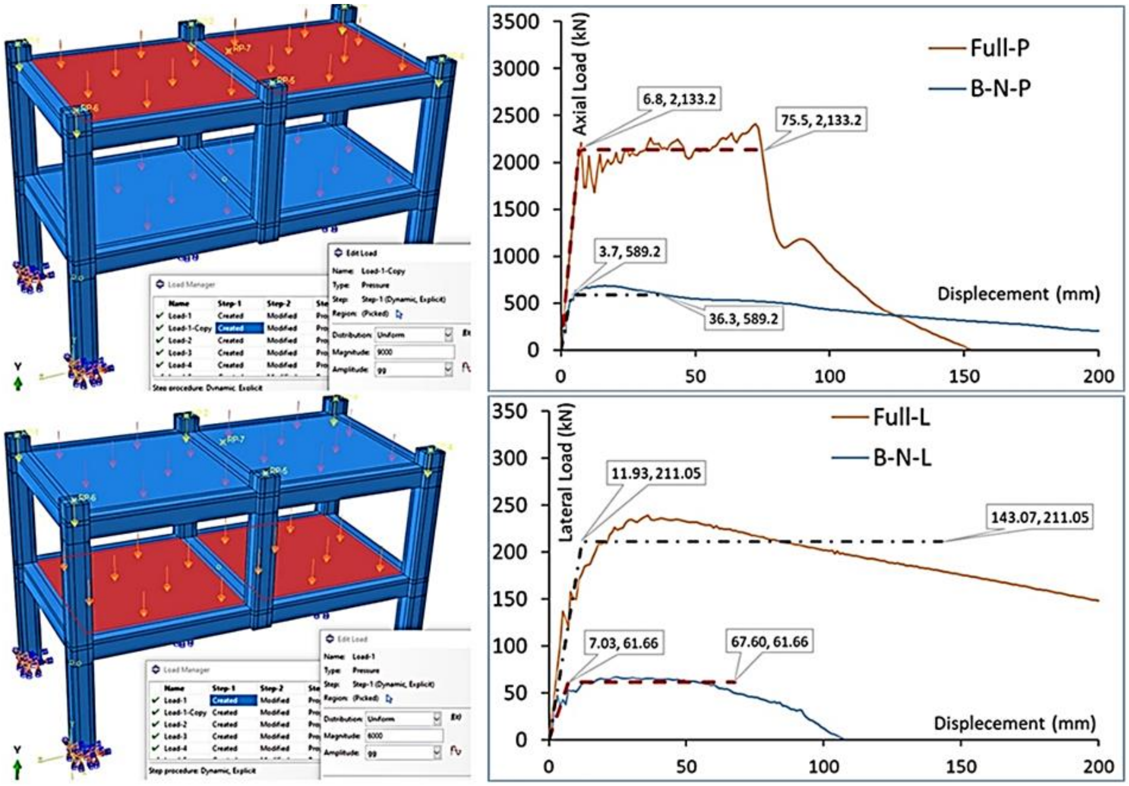

Figure 12. Comparison of vertical and lateral load-displacement curves in the two-story RC moment-resisting frame, under non-uniform mass load distribution, before and after removal of Column B.

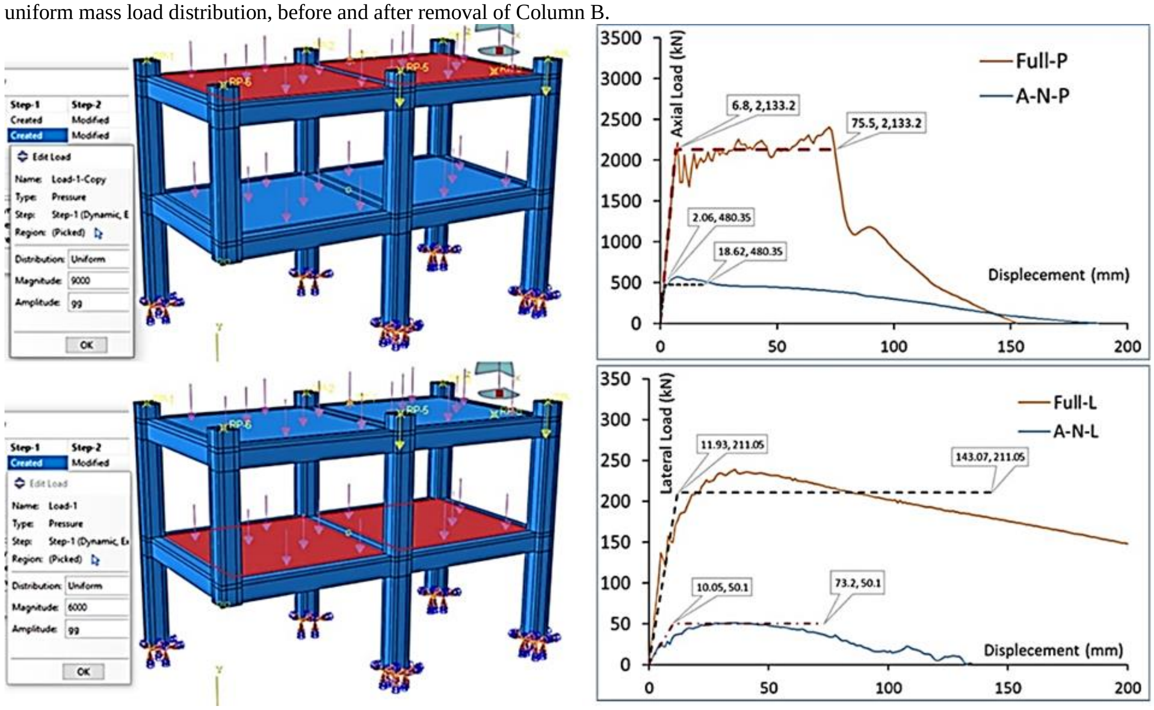

Figure 13. Comparison of vertical and lateral load-displacement curves in the two-story RC moment-resisting frame, under non-uniform mass load distribution, before and after removal of Column A.

3.4. Performance Evaluation and Sensitivity Index under Non-Uniform Mass Load Distribution due to Removal of Column A

Under the non-uniform mass distribution scenario associated with the removal of Column A, the structural performance and sensitivity index of the two-story RC moment-resisting frame were evaluated under both vertical and lateral loading. After applying the corresponding loads and analyzing the resulting load–displacement curves, the sensitivity index was calculated as 76.2% for vertical loading and 78.5% for lateral loading. Figure 13 compares the pre- and post-removal responses under critical loading, where A-N-P and A-N-L denote the vertical and lateral load–displacement behaviors, respectively, following the removal of Column A.

4. Results Evaluation

The analysis of the applied loads and resulting damage indicates that, during column removal and subsequent progressive collapse, compressive forces in adjacent columns exceed the original load of the removed column due to indirect gravity load transfer through surrounding beams and columns. The load–displacement resistance beneath the removed column is governed by the capacity of adjacent beams and slabs, exhibiting combined linear and nonlinear behavior, with the peak resistance defining the critical load. This critical load consists of both gravity loads from upper stories and dynamic effects associated with sudden column loss, and it plays a decisive role in collapse progression. Once this load is applied, significant structural damage develops, and further loading leads to propagation of progressive collapse toward the removed column, affecting adjacent beams and columns accordingly.

The collected analytical results for all modeled scenarios are summarized in Table 5 and Table 6, which reports the sensitivity indices as well as the vertical and lateral performance parameters of each frame configuration under both regular and irregular mass distributions.Review of Table 5 and Table 6 indicates that, in the two-story RC moment-resisting frame, corner columns exhibit substantially higher sensitivity to both vertical and lateral loading compared to side columns, with this effect amplified under irregular mass distribution. This trend is consistent across all loading conditions, underscoring the critical role of corner columns in progressive collapse resistance.In this study, the vertical and lateral performance of a two-story RC moment-resisting frame under regular and irregular mass loading was evaluated. The results indicate that the intact models (Full-P and Full-L) exhibit superior structural performance—including higher strength, stiffness, ductility, and energy absorption—compared with the models in which a column was removed. This demonstrates the significant reduction in structural capacity associated with column loss and its impact on progressive collapse behavior.The energy absorption results show that the removal of corner columns (A-M and B-M) under regular mass distribution leads to greater energy dissipation than the removal of side columns (A-N and B-N) under irregular loading, in both vertical and lateral directions. Furthermore, comparison of the remaining performance criteria—strength, stiffness, and ductility—indicates that irregular mass distribution consistently results in reduced structural capacity relative to the regular loading condition.

Table 5.
vertical performance and sensitivity index of a two-story RC moment-resisting frame under regular and irregular mass loading

Spectrum	Δ_y (mm)	Δ_u (mm)	E_p (kN·mm)	P_p (kN)	K_p (kN/mm)	μ_P	SI_P
Full-P	6.79	75.46	202843	2407.9	314.4	11.1	
A-N-P	2.06	18.62	54837	572.5	233.2	9.0	76.2%
B-N-P	3.66	36.30	55693	683.8	161.0	9.9	71.6%
A-M-P	3.05	32.00	84365	880.8	242.3	10.5	63.4%
B-M-P	3.46	35.26	74258	911.7	227.2	10.2	62.1%

Table 6.
lateral performance and sensitivity index of a two-story RC moment-resisting frame under regular and irregular mass loading

Spectrum	Δ_y (mm)	Δ_u (mm)	E_l (kN·mm)	P_l (kN)	K_l (kN/mm)	μ_L	SI_L
Full-L	11.93	143.1	38273	239.1	17.7	12.0	
A-N-L	10.05	73.2	4195	51.5	5.0	7.3	78.5%
B-N-L	7.03	67.6	5164	66.6	8.8	9.6	72.2%
A-M-L	9.01	73.2	5992	73.5	7.6	8.1	69.2%
B-M-L	6.948	0	6455	83.2	11.1	9.8	65.2%

5. Conclusion

This study examined the influence of mass irregularity on the stability and progressive collapse of reinforced concrete structures. Uneven floor mass distribution amplifies torsional effects and stress concentrations, increasing structural vulnerability, particularly under seismic loads. Mitigation strategies, including joint strengthening and optimized design, are therefore critical. Finite element analyses using ABAQUS demonstrated that maintaining uniform mass distribution and implementing advanced engineering solutions can significantly enhance structural resilience. The findings provide a framework for improving RC frame design and reducing the risk of progressive collapse.

1. The results indicate that during progressive collapse, adjacent columns experience higher loads than the removed column due to the redistribution of gravitational forces through surrounding beams and columns.
2. The vertical load–displacement response beneath a removed column reflects the capacity of adjacent beams and slabs, exhibiting an initial linear followed by nonlinear behavior up to the critical load. This critical load accounts for gravity from upper and same floors as well as dynamic effects from sudden column removal, highlighting the influence of load type and magnitude on progressive collapse. The sensitivity index further quantifies the significance of key structural elements under both vertical and lateral loading.
3. Applying the critical load to a removed column induces significant damage, particularly at beam ends, slab edges adjacent to the column, and the central diagonal region of the slab. Loads exceeding this threshold trigger progressive collapse, propagating toward the removed column and engaging surrounding structural elements.
4. Structural performance and sensitivity analyses indicate that corner-column removal poses a greater progressive collapse risk than side-column removal. Moreover, irregular mass distribution amplifies the sensitivity index, increasing vulnerability under both removal scenarios.
5. Performance analysis revealed that energy absorption is higher for corner-column removal than for side-column removal, while regular mass distribution enhances energy absorption compared to irregular loading. Strength, stiffness, and ductility similarly decrease under irregular loading.

This study concludes that column removal, particularly at corner locations, elevates the risk of progressive collapse due to the redistribution of gravity loads to adjacent beams and columns. Irregular mass distribution further increases structural sensitivity while reducing strength, stiffness, and ductility. Additionally, energy absorption is higher for corner-column removal compared to side-column removal.

References

[1] Paz, M., Leigh, W. (2004). Dynamic Analysis of Three-dimensional Frames. In: Structural Dynamics. Springer, Boston, MA. https://doi.org/10.1007/978-1-4615-0481-8_13.

[2] Biria, M. (2017). A review on Progressive Collapse of Steel Buildings. Journal of Civil Engineering Researchers, 1(3),14. https://www.journalsresearchers.com/ojs/index.php/jcer/article/view/14.

[3] Fallah, M. (2021). Research and Practice on Progressive Collapse and Building Strength in 2019 and 2020. Journal of Civil Engineering Researchers, 3(3), 13-21. https://www.journals-researchers.com/ojs/ index.php/jcer/article/view/44.

[4] El-Sheikh, M. M., Elsanadedy, M. A., Alabdulhady, Y. A., Ashour, A. F. (2021). Progressive collapse of structures: Current trends and future directions. Engineering Structures, 244, 112482. https://doi.org/10.1016/j.engstruct.2021.112482.

[5] Starossek, U., Haberland, M. (2011). Disproportionate Collapse: Terminology and Procedures. Journal of Performance of Constructed Facilities, 25(6), 516–525. https://doi.org/10.1061/(ASCE)CF.1943-5509.0000138.

[6] Alshami, A. A., Jalloul, H., Merrick, D., Hart, L., Choi, J., Manheim, D., Yesiller, N. (2021). SUstainable Material Management Extreme Events Reconnaissance (SUMMEER).

[7] Pearson, C., Norbert, A. (2012). Lessons from the Progressive Collapse of the Ronan Point Apartment Tower. Forensic Engineering, 2003. https://doi.org/10.1061/40692(241)21.

[8] Chopra, A. K., Chintanapakdee, C. (2004). Inelastic deformation ratios for design and evaluation of structures: Single-degree-of-freedom bilinear systems. Journal of Structural Engineering, 130(9), 1309–1319. https://doi.org/10.1061/(ASCE)0733-9445(2004)130:9(1309).

[9] Kabeyasawa, T., Kim, J., Kim, T. (2009). Progressive Collapse Simulation of Reinforced Concrete Buildings Using Column Models with Strength Deterioration after Yielding. In: Improving the Seismic Performance of Existing Buildings and Other Structures. https://doi.org/10.1061/41084(364)47.

[10] Mohamed, O. A. (2010). Effect of mass irregularity on structural progressive collapse. Proceedings of the 9th U.S. National and 10th Canadian Conference on Earthquake Engineering. Toronto, Canada.

[11] Jankowiak, T., Ziemiański, L., Ziółkowski, M. (2013). Sensitivity analysis of RC frames to mass irregularities. Archives of Civil and Mechanical Engineering, 13(4), 518–528. https://doi.org/10.1016/j.acme.2013.07.005.

[12] Nouri, G., Yosefzaei, M. R. (2020). Effect of Mass Irregularity on the Progressive Collapse Potential of Steel Moment Frames. In: Köber, D., De Stefano, M., Zembaty, Z. (eds) Seismic Behaviour and Design of Irregular and Complex Civil Structures III.

Geotechnical, Geological and Earthquake Engineering, vol 48. Springer, Cham. https://doi.org/10.1007/978-3-030-33532-8_27.

[13] Bai, Y., Li, Y., Tang, Z. (2021). Seismic collapse fragility of low-rise steel moment frames with mass irregularity based on shaking table test. Bulletin of Earthquake Engineering, 19, 2457–2482. https://doi.org/10.1007/s10518-021-01076-2.

[14] Ghanem, A., Lee, S. M. Y.-J., (2023). Seismic Vulnerability of Reinforced Concrete Frame Structures: Obtaining Plan or Vertical Mass Irregularity from Structure Use Change. Journal of Structural Engineering, 150(3). https://doi.org/10.1061/JSENDH.STENG-12440.

[15] Ghimire, K., Chaulagain, H. (2021). Common Irregularities and Its Effects on Reinforced Concrete Building Response. Structural Mechanics of Engineering Constructions and Buildings.

[16] Liu, C., Zhang, S., Zhang, D., Wang, Z. (2023). Model tests on progressive collapse mechanism of a shallow subway tunnel in soft upper and hard lower composite strata. Tunnelling and Underground Space Technology, 131, 104824. https://doi.org/10.1016/j.tust.2022.104824.

[17] Lekshmi, N. H., Aswathy, S. Kumar. (2013). Dynamic Analysis of an Irregular RC Building with Different Bracing Systems. International Journal of Science and Research (IJSR). ISSN: 2319-7064.

[18] Zhang, R., Soong, T. T. (1992). Seismic design of viscoelastic dampers for structural applications. Journal of Structural Engineering, 118(5), 1375–1392. https://doi.org/10.1061/(ASCE)0733-9445(1992)118:5(1375).

[19] Christopoulos, C., Filiatrault, A. (2006). Principles of Passive Supplemental Damping and Seismic Isolation. IUSS Press.

[20] Spencer Jr, B. F., Nagarajaiah, S. (2003). State of the art of structural control. Journal of Structural Engineering, 129(7), 845–856. https://doi.org/10.1061/(ASCE)0733-9445(2003)129:7(845).

[21] Chopra, A. K. (2017). Dynamics of Structures: Theory and Applications to Earthquake Engineering (5th ed.). Pearson Education.

[22] Lignos, D. G., Krawinkler, H. (2012). Deterioration Modeling of Steel Components in Support of Collapse Prediction of Steel Moment Frames under Earthquake Loading. Journal of Structural Engineering, 138(3), 397–408. https://doi.org/10.1061/(ASCE)ST.1943-541X.0000376.

[23] Kewalramani, M. A., Syed, Z. I. (2018). Seismic analysis of torsional irregularity in multi-storey symmetric and asymmetric buildings. Eurasian Journal of Analytical Chemistry, 13, 286–292.

[24] Huang, H., Huang, M., Zhang, W., Guo, M., Liu, B. (2021). Progressive collapse of multistory 3D reinforced concrete frame structures after the loss of an edge column. Structure and Infrastructure Engineering. https://doi.org/10.1080/15732479.2020.1841245.

[25] Dassault Systèmes Simulia Corp. (2015). ABAQUS/Standard Theory Manual, ABAQUS-V6.16-1. Johnston, RI, USA.